The influence of the cloud shell on tracer budget measurements of LES cloud entrainment

JORDAN T DAWE * AND PHILIP H AUSTIN

Department of Earth and Ocean Sciences, University of British Columbia, Vancouver, BC, Canada.

*Corresponding author address: Jordan T Dawe, Department of Earth and Ocean Sciences, University of British Columbia, 6339 Stores Road, Vancouver, BC, V6T 1Z4, Canada.

E-mail: jdawe@eos.ubc.ca

ABSTRACT

Direct measurements of rates of entrainment into and detrainment from cumulus cloud cores obtained from LES model cloud fields produce values twice as large as those produced from tracer budget calculations. This difference can be explained by two effects: the presence of a shell of moist air around the cloud cores and drier air at the edge of the cloud core, and the tendency for the mean tracer value of the entrained fluid to be greater than the mean tracer value of the cloud shell. Preferential entrainment of shell air that is moving upward faster than the mean shell creates strong vertical momentum fluxes into the cumulus cloud core, making the assumption that cumulus clouds entrain fluid with zero vertical momentum incorrect. Variability in the properties of the moist cloud shell has strong impacts on entrainment values inferred from tracer budget calculations. These results indicate the dynamics of the cloud shell should be included in parametrization of cumulus clouds used in general circulation models.

1. Introduction

The rate at which air is entrained into and detrained from cumulus clouds affects cloud properties, cloud top height, and vertical transports of heat and moisture. Proper simulation of cumulus sub-grid scale fluxes in General Circulation Models (GCM) depends on the accurate parametrization of entrainment of environmental tracer properties into the clouds and detrainment of cloud properties into the environment (Bechtold et al. 2008; de Rooy and Siebesma 2010).

Entrainment and Detrainment may be defined mathematically as

$$E = -\frac{1}{A} \oint_{\hat{\mathbf{n}}\cdot(\mathbf{u}-\mathbf{u_i})<0} \rho\hat{\mathbf{n}} \cdot (\mathbf{u} - \mathbf{u_i})dl \tag{1a}$$

$$D = \frac{1}{A} \oint_{\hat{\mathbf{n}}\cdot(\mathbf{u}-\mathbf{u_i})>0} \rho\hat{\mathbf{n}} \cdot (\mathbf{u} - \mathbf{u_i})dl \tag{1b}$$

1   where E and D are the entrainment and detrainment rates in kg m^{-3} s^{-1}, ρ is the density of

2   air in kg m^{-3} s^{-1}, $\mathbf{u}$ is the velocity of the air in m s^{-1}, $\mathbf{u_i}$ is the velocity of the cloud surface

3   in m s^{-1}, A is the area of the cloud in m^2, $\hat{\mathbf{n}}$ is a unit vector directed out the cloud surface,

4   and the path integral is taken around the cloud surface at a constant vertical level (Siebesma

5   1998). Entrainment and detrainment are thus caused by differences between the motion of

6   the cloud surface and the motion of the air. This includes not just mixing processes, but

7   also adiabatic processes such as condensation of fluid at cloud base. Many parameterizations

8   use cloud core as the region over which to consider entrainment and detrainment, defined as

9   regions having condensed liquid water, positive buoyancy, and upward vertical velocity. In

10 this case, the motion of the cloud core surface is simply substituted for the motion of the

11 cloud surface in equations (1).

Entrainment and detrainment rates impact GCM parameterizations in several ways. First, profiles of cloud vertical mass flux are usually calculated from parametrized entrainment values using the continuity equation for a simple entraining plume to represent an ensemble of cumulus clouds:

$$\rho\frac{\partial a}{\partial t} + \frac{\partial M_{core}}{\partial z} = E - D. \tag{2}$$

12 Here a is the fractional cloud core area and M_{core} is vertical cloud core mass flux (kg m^{-2}

13 s^{-1}). The level where the mass flux profile goes to zero then defines the location of the cloud

14 ensemble top. This mass flux profile is combined with the entrainment rate of environmental

2

air into the cloud and the detrainment rate of cloud air into the environment to generate
vertical profiles of cloud water vapor, condensate, and temperature, and these profiles are
then used to calculate the moistening of the environment by detrainment of cloud fluid
(Tiedtke 1989; Kain and Fritsch 1990). Precipitation rates are also generated from the
mass flux and tracer profiles produced from the entrainment and detrainment profiles. This
wide variety of effects make entrainment rate one of the strongest controls on the climate
sensitivity of GCMs (Stainforth et al. 2005; Rougier et al. 2009).

Large Eddy Simulation (LES) is the primary tool used to study cloud entrainment. LES
mass entrainment and detrainment rates are typically obtained using budgets of conserved
tracer variables to infer the amount of fluid exchange between the cloud ensemble and the
surrounding air. Siebesma and Cuijpers (1995) derive the following equations for entrainment
and detrainment of mass from the ensemble of cloud core plumes:

$$E_\phi(\phi_{core} - \phi_{env}) = -M_{core}\frac{\partial \phi_{core}}{\partial z} - \frac{\partial \rho a \overline{w'\phi'}^{core}}{\partial z} - \rho a \frac{\partial \phi_{core}}{\partial t} + a\rho \left(\frac{\partial \bar{\phi}}{\partial t}\right)_{forcing} \tag{3a}$$

and

$$D_\phi(\phi_{core} - \phi_{env}) = -M_{core}\frac{\partial \phi_{env}}{\partial z} + \frac{\partial \rho (1-a) \overline{w'\phi'}^{env}}{\partial z} + \rho(1-a)\frac{\partial \phi_{env}}{\partial t} - \rho(1-a)\left(\frac{\partial \bar{\phi}}{\partial t}\right)_{forcing} \tag{3b}$$

Where ϕ (with units denoted by $[\phi]$) represents any conserved tracer, such as the total spe-
cific humidity q_t (kg water kg^{-1} moist air) or the liquid-water moist static energy h (J kg^{-1});
w is vertical velocity (m s^{-1}); *env* and *core* sub-and super-scripts denote horizontally aver-
aged values conditionally sampled in the cloud environment and core; *forcing* refers to tracer
sources and sinks, such as radiation or large-scale subsidence, not included in the other terms;
primed values represent anomalies relative to the horizontal mean; overbars represent hori-

3

zontal averaging; and $E_\phi(z)$ and $D_\phi(z)$ are the total mass entrainment into and detrainment from the cloud core inferred from the tracer budget, in kg s^{-1} m^{-3}. Under this budget formulation, $E_\phi(z)$ and $D_\phi(z)$ consist of all horizontal mass exchanges between clouds and their environment, including advective processes, diffusive processes, and thermodynamic phase changes. We shall refer to values calculated by this method as "tracer budget" entrainment and detrainment. For convenience, the various tracer and entrainment/detrainment rate subscripts used below are summarized in the Appendix.

Alternatively, entrainment and detrainment of mass can be calculated directly from the LES velocity and tracer fields. Romps (2010) recently presented a technique to measure local (grid scale) mass entrainment $e(x, y, z)$ and detrainment $d(x, y, z)$. His equation (2) is:

$$e - d = \frac{\partial}{\partial t}(\mathcal{A}\rho) + \nabla \cdot (\rho \mathbf{u} \mathcal{A}) \tag{4}$$

Here $\mathcal{A}$ is the "activity" of the fluid, where $\mathcal{A}$ is one at cloud core points and zero otherwise. The values of $e - d$ are averaged over the time that a grid cell experiences mass fluxes between an active and an inactive point, then positive $e - d$ values are considered to be purely e, and negative values, d. Summing these point measurements horizontally gives $E_d(z)$ and $D_d(z)$, the total mass entrained into and detrained from the cloud core field in kg s^{-1} m^{-3}, where the d subscript indicates these quantities were calculated directly from the model velocity and tracer fields. We shall refer to entrainment and detrainment values calculated by this method as "direct" entrainment and detrainment.

Romps found that such direct calculation of the entrainment and detrainment mass fluxes produced values roughly twice as large as tracer budget calculations. Romps attributed this difference to the tracer budget calculation assumption that fluid exchanged between

4

clouds and environment has the mean properties of the cloud or environment at that level, respectively. Studies of the dense, descending shell of moist air that forms around trade-wind cumulus clouds (Jonas 1990; Rodts et al. 2003; Heus and Jonker 2008; Jonker et al. 2008; Heus et al. 2009; Wang and Geerts 2010) suggest that the cloud shell properties are quite different than the core or environment properties, bolstering Romps' hypothesis. Since fluid exchanges between clouds and environment must pass through this shell, it is likely that it plays an important role in entrainment and detrainment dynamics.

Below we examine the sources of the discrepancy in entrainment and detrainment values calculated via tracer budgets and directly using (4). We show that the discrepancy is explained by two effects: the presence of the shell of moist air around the cloud cores and drier air at the edge of the cloud core, and preferential entrainment of shell air with higher average humidity and upward velocity than the mean shell properties which enhances tracer fluxes between the clouds and the environment. We derive a relation to transform the direct mass entrainment and detrainment fluxes into tracer budget values suitable for use in one-dimensional simple entraining plume cloud parameterizations, and then use these transformed fluxes to evaluate the impact of the shell on tracer budget entrainment and detrainment rates of specific humidity and vertical velocity. Finally, we examine the dynamics that drives the preferential entrainment of air with higher than average specific humidity and vertical velocity.

2. Model description

All LES calculations in this paper were made using the System for Atmospheric Modeling (SAM; Khairoutdinov and Randall 2003). Two model runs were performed, configured as standard Global Energy and Water Cycle Experiment (GEWEX) Cloud System Studies (GCSS; Randall et al. 2003) experiments: a Barbados Oceanographic and Meteorological Experiment (BOMEX; Siebesma et al. 2003) run, and an Atmospheric Radiation Measurement Study (ARM; Brown et al. 2002) run. The BOMEX run was performed on a 6.4 km x 6.4 km horizontal x 3.2 km vertical domain with 25 meter grid size in all directions for 6 hours, and the first three hours of simulation were discarded. The ARM run was performed on a 7.68 km x 7.68 km x 4.5 km domain with 30 meter grid size. Precipitation was disabled in both runs.

We have implemented the direct entrainment calculation scheme of Romps (2010) in SAM, allowing us to calculate the mass of air entrained into and detrained from cloud core directly from model ρ, $\mathbf{u}$, and $\mathcal{A}$. Romps (2010, eq. 4) also presents a method for calculating local entrainment and detrainment rates for any model variable in the same framework as (4), but neglects forcing terms. These terms are significant for quantities like vertical momentum, so we modify Romps' equation to include their effects:

$$e\phi - d\phi = \frac{\partial}{\partial t}(\phi\mathcal{A}\rho) + \nabla \cdot (\phi\rho\mathbf{u}\mathcal{A}) - \rho\mathcal{A}S_\phi. \tag{5}$$

where S_ϕ is any non-advective and non-diffusive source or sink term for ϕ, such as precipitation for q_t or pressure gradient for w, in units of $[\phi]$ s^{-1}. Diffusion is excluded from S_ϕ as it is part of the entrainment/detrainment process, and so is included in the $e\phi - d\phi$ term of the equation. The inclusion of these source/sink terms allows us to expand the definition of

¹ ϕ to include non-conserved fluid properties.

² As with equation (4), the local $(e\phi)(x, y, z)$ and $(d\phi)(x, y, z)$ must be horizontally summed

³ to give the total entrainment into or detrainment out of the cloud ensemble for any fluid

⁴ property, but since ϕ can be negative for properties like vertical velocity, it is possible for

⁵ entrainment to reduce and for detrainment to increase the various properties of the cloud

⁶ core. To accommodate this effect, if the average value of ϕ is positive over the time that a grid

⁷ cell experiences mass fluxes between an active and an inactive grid cell, then positive $e\phi - d\phi$

⁸ values are considered to be purely $e\phi$, and negative values, $d\phi$. However, if the average of

⁹ ϕ is negative, then positive $e\phi - d\phi$ values are considered to be purely $(d\phi)(x, y, z)$, and

¹⁰ negative values, $(e\phi)(x, y, z)$.

¹¹ The obvious way to calculate the average value of ϕ is to perform a flux-weighted calcu-

¹² lation, so that $\phi = (e\phi - d\phi)/(e - d)$. However, doing so for positive definite quantities, such

¹³ as total specific water q_t, sometimes results in negative ϕ. To see the reason for this, consider

¹⁴ a situation where $(e - d)$ integrated over the period that a grid cell is active is found to be

¹⁵ slightly bigger than zero for a grid cell. The Romps algorithm would assign e to a small

¹⁶ value and d to be zero, but this is only one of many equally valid choices; as long as $e \approx d$,

¹⁷ the net flux measured by the algorithm would be satisfied. At the same time, $(eq)_d - (dq)_d$

¹⁸ $((e\phi)_d - (d\phi)_d$ using q_t for $\phi)$ is found to be negative, presumably due to e and d having

¹⁹ similar magnitudes while the detraining air has higher humidity than the entraining air. In

²⁰ this case, $((eq)_d - (dq)_d)/(e - d)$ will be negative, even though q_t is always positive. To

²¹ avoid this problem, we calculate ϕ as a simple time average for the purpose of determining

²² if $e\phi - d\phi$ is assigned to $e\phi$ or to $d\phi$. Horizontal summation of $(e\phi)$ and $(d\phi)$ then gives

²³ $(E\phi)_d(z)$ and $(D\phi)_d(z)$, the total entrainment and detrainment of a property for the cloud

7

ensemble in units of $[\phi]$ kg s^{-1} m^{-3} calculated directly from the model velocity and property fields.

3. Relationship Between Direct and Tracer Budget Entrainment

Romps (2010) established that the direct estimate of mass entrainment and detrainment yields values roughly twice the size of those calculated via conserved tracer budgets. Furthermore, examination of the ratios of the mass entrainment and detrainment calculated via a total specific water budget (E_q, D_q) to the directly calculated values (E_d, D_d) over the diurnal cycle of an ARM LES reveals significant changes over the course of the day (Fig. 1). Thus, the direct and tracer budget measurements of E and D are not only significantly different, but have differing dynamics, which may need to be be accounted for in large-scale parameterizations of cloud entrainment and detrainment. In this section we examine the sources of disagreement between direct and tracer budget estimates of mass entrainment into and detrainment from the cloud core.

a. E and D Cloud Shell Correction

Romps attributed the differences between (E_ϕ, D_ϕ) and (E_d, D_d) to the assumption made by Siebesma and Cuijpers (1995) that fluid being entrained or detrained has the properties of the mean environment or cloud core, respectively. If we examine the horizontal mean specific humidity of the fluid at the "cloud core edge" (cloud core model grid cells that are

8

nearest-neighbor adjacent to non-core cells), which presumably is the fluid being detrained, we see it is indeed drier than the mean core (Fig. 2a). Similarly, the fluid available for entrainment in the "cloud core shell" (non-core model grid cells that are nearest-neighbor adjacent to core cells) is moister than the mean environment.

Budget equations that explicitly distinguish between the mean cloud core and environment properties and the properties of the entraining and detraining fluid allow us to transform (E_d, D_d) values into equivalent tracer budget values, and back again. We start our derivation with the observation that both the tracer budget and direct values of E and D are consistent with the continuity equation (equations (2) and (4)). This implies

$$E_\phi - D_\phi = E_d - D_d. \tag{6}$$

Similarly, the entrainment and detrainment rates of fluid properties must be consistent with the total property budget, giving us

$$E_\phi \phi_{env} - D_\phi \phi_{core} = E_d \phi_E - D_d \phi_D, \tag{7}$$

where ϕ_E and ϕ_D represent the ϕ of the fluid being entrained or detrained, respectively. Combining these equations and solving for E_ϕ and D_ϕ in turn results in:

$$E_{\phi,T} = E_d - \left[E_d \frac{(\phi_E - \phi_{env})}{(\phi_{core} - \phi_{env})} + D_d \frac{(\phi_{core} - \phi_D)}{(\phi_{core} - \phi_{env})} \right] \tag{8a}$$

$$D_{\phi,T} = D_d - \left[E_d \frac{(\phi_E - \phi_{env})}{(\phi_{core} - \phi_{env})} + D_d \frac{(\phi_{core} - \phi_D)}{(\phi_{core} - \phi_{env})} \right]. \tag{8b}$$

Here the T subscript indicates these E_ϕ and D_ϕ tracer budget values have been calculated by transformation of direct values, not via equations (3). The bracketed terms represent the bias introduced by assuming that entrained/detrained air has the properties of the mean

9

environment and core. Thus, to convert from (E_d, D_d) to $(E_{\phi,T}, D_{\phi,T})$, both E_d and D_d

must be reduced by $E_d A + D_d B$, where $A = (\phi_E - \phi_{env})/(\phi_{core} - \phi_{env})$ and $B = (\phi_{core} - \phi_D)/(\phi_{core} - \phi_{env})$.

Note that rearrangement of A gives $\phi_E = A\phi_{core} + (1 - A)\phi_{env}$, meaning that A can be

thought of as the fraction of mean core air in a mixture of mean core and mean environment

air needed to produce the properties of the entrained fluid. Similarly, $\phi_D = B\phi_{env} + (1 - B)\phi_{core}$ and B can be thought of as the fraction of mean environment air in a mixture of

mean core and mean environment air needed to produce the properties of the detrained

fluid. Since the fluid being entrained or detrained does not necessarily originate at the level

it is entrained or detrained at, we cannot assume that a fraction A of the entrained air is

modified core air. Nevertheless, A and B are likely related to the recirculation of entrained

and detrained air.

Alternatively, we can solve for E_d and D_d, arriving at

$$E_{d,T} = E_\phi + \left[E_\phi \frac{(\phi_E - \phi_{env})}{(\phi_D - \phi_E)} + D_\phi \frac{(\phi_{core} - \phi_D)}{(\phi_D - \phi_E)} \right]. \tag{9a}$$

$$D_{d,T} = D_\phi + \left[E_\phi \frac{(\phi_E - \phi_{env})}{(\phi_D - \phi_E)} + D_\phi \frac{(\phi_{core} - \phi_D)}{(\phi_D - \phi_E)} \right]. \tag{9b}$$

Again, the T subscript indicates these E_d and D_d values have been calculated by transfor-

mation of E_ϕ and D_ϕ, not via equation (4). In this case, to convert from (E_ϕ, D_ϕ) to $(E_{d,T}, D_{d,T})$, both E_ϕ and D_ϕ must be increased by $E_\phi a + D_\phi b$, where $a = (\phi_E - \phi_{env})/(\phi_D - \phi_E)$

and $b = (\phi_{core} - \phi_D)/(\phi_D - \phi_E)$.

We now have relationships allowing us to transform the unbiased E_d and D_d values

into biased tracer budget E_ϕ and D_ϕ values, which are better suited for simple entraining

plume parametrization of cloud fields. Comparison of E_q and D_q (E_ϕ and D_ϕ inferred using

10

1 total specific moisture q_t as the tracer) with E_d and D_d shows the direct entrainment and

2 detrainment magnitudes are significantly larger than the tracer budget values (Figure 2b

3 and 2c, grey and dotted lines). Using (8) to calculate $E_{q,T}$ and $D_{q,T}$ with $q_E = q_{edge}$, the

4 horizontal mean humidity in the cloud edge, and $q_D = q_{shell}$, the horizontal mean humidity

5 in the cloud shell, results in values quite close to the tracer budget values above the middle

6 of the cloud layer. The transformation also duplicates the negative detrainment values near

7 cloud base that are typically produced by tracer calculations.

8 *b. Preferential Entrainment of Moist, Ascending Air*

9 Relative to the tracer budget values, the $E_{q,T}$ and $D_{q,T}$ values calculated using $q_E = q_{edge}$

10 and $q_D = q_{shell}$ are still too large near cloud base. We can explain this difference as being the

11 result of the mean fluid property values of the entrained and detrained air being different

12 than the mean value of the shell and edge air, respectively. Using the mean shell and edge

13 values of properties to transform the direct entrainment and detrainment assumes that any

14 fluid parcel in the shell or edge is equally likely to be entrained or detrained. In reality,

15 mixing relatively dry air into the cloud core is more likely to cause evaporation, which will

16 drive detrainment, while mixing relatively moist air into the cloud core is more likely to

17 produce a saturated fluid mixture, resulting in entrainment. This suggests that the moistest

18 shell parcels are more likely to undergo entrainment than the average shell parcel, and the

19 driest edge parcels are more likely to detrain than the average edge parcel.

20 We can directly calculate the effective fluid property values at which entrainment occurs

21 by taking the total fluid property entrainment $(E\phi)_d$ (calculated via equation (5)) and divid-

11

ing it by the total mass entrainment E_d so that $\phi_{entrain} = (E\phi)_d/E_d$. Similarly, the effective

property values of the detraining air can be found from $\phi_{detrain} = (D\phi)_d/D_d$. Examination

of these values from the BOMEX simulation using q_t for ϕ shows $q_{entrain}$ is moister than

q_{shell} (Figure 3a), indicating entrainment occurs preferentially at the moistest parts of the

shell. Conversely, there is little difference between between $q_{detrain}$ and q_{edge}, indicating the

detrained parcels tend to have the mean moisture of the cloud core edge. Using $q_{entrain}$ and

$q_{detrain}$ to transform E_d and D_d reduces the large entrainment and detrainment values near

cloud base found using the mean shell and edge properties (solid black line, Fig. 3b and 3c),

bringing $E_{q,T}$ and $D_{q,T}$ into agreement with E_q and D_q.

4. E_q, E_h and E_w Differences

Equations (8a) or (8b) imply that the tracer budget method will measure different entrainment and detrainment values for fluid properties with differing values of $A = (\phi_E - \phi_{env})/(\phi_{core} - \phi_{env})$ and $B = (\phi_{core} - \phi_D)/(\phi_{core} - \phi_{env})$. With this in mind we compare transformed $E_{\phi,T}$ and $D_{\phi,T}$ values produced by liquid water moist static energy h and vertical velocity w with those produced using total specific moisture q_t.

Liquid water moist static energy shows a similar relative distribution of core, edge, shell, environment, entrained, and detrained properties when compared to q_t, indicating a tight coupling between these variables in the cloud dynamics. Because these properties are so tightly coupled, $E_{h,T}$ and $D_{h,T}$ values are nearly identical to the $E_{q,T}$ and $D_{q,T}$ (not shown).

Vertical velocity shows very different relative profiles compared to q_t or h (c.f. Fig. 4a and Fig. 3a). There is a much wider spread in the w values, with the shell having nearly zero

12

vertical velocity and the edge being halfway between the core and the environment. $w_{detrain}$
is slightly larger than the value of w in the cloud core edge, while $w_{entrain}$ is much larger
than w in the shell, becoming roughly the same value as w_{edge}. Since $w_{entrain}$ and $w_{detrain}$
are both larger than w_{shell} and w_{edge} this implies that rapidly rising air is both preferentially
entrained and detrained over slowly rising air. These effective entrainment and detrainment
w values produce $E_{w,T}$ and $D_{w,T}$ values (solid black line, Fig. 4c and Fig. 4c) that are quite
different than the transformed entrainment and detrainment produced by q_t and h (dotted
line, Fig. 4b and 4c); $E_{w,T}$ is negative near cloud base while $E_{q,T}$ is positive, and both $E_{w,T}$
and $D_{w,T}$ are half the magnitude of $D_{q,T}$ over much of the cloud layer.

Finally, we examine the temporal variability of $A = (\phi_E - \phi_{env})/(\phi_{core} - \phi_{env})$ and
$B = (\phi_{core} - \phi_D)/(\phi_{core} - \phi_{env})$ from the transformation equations (8a) and (8b) in the ARM
model run. Since A represents the fraction of core air in a mixture of core and environmental
air which has the properties of ϕ_E, and B represents the fraction of environmental air in
a mixture of core and environmental air which has the properties of ϕ_D, A and B provide
information about the amount of recirculation of entrained and detrained fluid occurring at
different model heights. However, A and B cannot be considered exact mixing fractions, as
the source heights of air mixtures may be different than the height at which they entrain
or detrain, and not all mixtures of core and environment properties are equally likely to
undergo entrainment.

A and B calculated for q_t both show strong changes over the ARM diurnal cycle (Figure
5, a and b). Near cloud base, A is nearly one while B is nearly zero, implying that both the
entrained and detrained air have the properties of the cloud core air. This is due to the main
entrainment process at cloud base being condensation of rising thermals instead of mixing;

buoyant updrafts simply condense without modification of their properties. Similarly, the air that detrains from the clouds at cloud base is almost undiluted because most entrainment at this level comes from the well-mixed sub-cloud layer below and so has properties nearly identical to the cloud core. At cloud top, A is also nearly one while B is nearly zero, implying that both the entrained and detrained air have the properties of the cloud core air. Here, this is due to the main detrainment process from the core being clouds becoming negatively buoyant as θ_v in the inversion increases faster than heating due to condensation can add buoyancy to the cloud core (Wu et al. 2009). Since this process does not depend on mixing, the air detraining from the core is relatively undiluted by the environment. Conversely, much of the air surrounding the remaining cloud core which is available for entrainment was previously detrained from the core without mixing, and so has the properties of the core air.

As the clouds mix into the inversion over the course of the day, they cause the inversion to rise. This means that points in the mid-cloud layer are less influenced by the adiabatic entrainment and detrainment processes occurring at cloud base and cloud top, and so the effects of mixing become more prominent. By the end of the day, A within the cloud layer has values near 0.6, suggesting that a significant amount of re-entrainment of air previously detrained from the core still occurs. B has values near 0.2, indicating that air detraining from the core is relatively undiluted by environmental air; this makes sense, since relatively little dilution by environmental air is required to cause the core air to become neutrally buoyant and detrain.

When calculated for w, A reaches a value around 0.4 and B goes to 0.6. The difference between these values and the values of A and B calculated for q_t is the result of buoyancy and pressure gradient forces on the mixtures, and the stronger tendency for upward-moving

14

shell parcels to be entrained relative to the tendency to entrain moister shell parcels. In other words, a relatively dry, rapidly ascending shell parcel is more likely to be entrained than a relatively moist, slowly ascending shell parcel. This is especially apparent near cloud base where the values of A are larger than 1, due to the mean entrained parcels having a larger upward velocity than the mean core parcels.

Performing these calculations with fixed values of $(\phi_{core} - \phi_{env})$, to remove changes due to movement of the mean environment and core profiles, shows similar results. Changes in the properties of the entraining and detraining fluid due to the dynamics of mixing and entrainment in the shell clearly are active in determining the rates at which properties entrain and detrain.

5. Causes of Preferential Entrainment of Moist, Ascending Air

The reason that shell air which is moister and ascending faster than the mean shell is more likely to be entrained can be seen by comparing instantaneous snapshots of the model values of local mass entrainment e, moisture entrainment eq_t, and vertical velocity entrainment ew. Since the Romps (2010) method of calculating e and d requires taking time averages, it is unsuitable for calculating instantaneous entrainment fields. Instead, we use an alternative method we have devised that substitutes spatial interpolation for time averaging (Dawe and Austin 2011). This alternative method results in slightly smaller values of e and d than those produced by Romps' method, but the two calculations show good agreement in variability.

15

The eq_t and ew fields are calculated simply by multiplying the value of e by the values of q_t and w, respectively.

Comparing the e, eq_t, and ew fields shows that e and eq_t have a very similar spatial pattern, but ew is concentrated in regions where strong updrafts enter the cloud core (Figure 6). The reason for this can been seen by examining the buoyancy, condensed liquid water, and vertical velocity fields that define the cloud core. Of these three fields, buoyancy is the strongest constraint determining if air is part of the core. However, regions exist far above cloud base where air has become negatively buoyant but maintains upward velocity and condensed liquid water. As this air continues to rise more condensation occurs, which heats the updraft, makes it positively buoyant, and thus entrains it into the core. In this way, entrainment is positively correlated with both q_t and w. This process occurs fairly often in our model cloud field, as evidenced both by our manual examination of the output fields, and the size of the difference between w_{shell} and $w_{entrain}$ in the mean profiles.

6. Discussion

Considering all these results, we now turn to the most important question of all: which entrainment value is the right one? The unsatisfying answer is that it depends on the purpose for which the entrainment is to be used.

Consider a cumulus cloud parametrization based upon a simplified form of the continuity equation which assumes the cloud fraction is constant,

$$\frac{\partial M_{core}}{\partial z} = E - D \tag{10}$$

16

a cloud budget equation that assumes mean vertical advection is balanced by entrainment of mean environmental properties,

$$M_{core}\frac{\partial \phi_{core}}{\partial z} = E(\phi_{env} - \phi_{core}) \tag{11}$$

and a simple detrainment forcing equation,

$$\rho\frac{\partial \phi_{env}}{\partial t} = D(\phi_{core} - \phi_{env}). \tag{12}$$

1   ϕ_{env} is input to the parametrization from the GCM. If we assume we have a perfect parametriza-

2   tion of M_{core} and ϕ_{core} at cloud base with which to construct mean core mass flux and tracer

3   profiles, we wish the E and D values to produce a profile of $\partial\phi_{core}/\partial t$ to force the GCM

4   which agrees with LES results for a similar mean environmental profile. The E and D we

5   desire then is closer to E_ϕ and D_ϕ than E_d and D_d, but nevertheless must be modified to

6   account for the time tendency and Reynolds flux budget terms we have neglected. This

7   also implies that we should have different E_ϕ and D_ϕ values for properties with different

8   distribution patterns around the clouds.

Using values near E_d and D_d instead would require modifying equation (11) to become

$$M_{core}\frac{\partial \phi_{core}}{\partial z} = E(\phi_{core} - \phi_E) - D(\phi_{core} - \phi_D) \tag{13}$$

and equation (12) into

$$\rho\frac{\partial \phi_{env}}{\partial t} = D(\phi_D - \phi_{env}) - E(\phi_E - \phi_{env}). \tag{14}$$

9   Now, instead of calculating different E and D values for each tracer we wish to model, we

10   must instead calculate ϕ_E and ϕ_D values for each property that is entrained or detrained.

11   While it is possible this would produce a better parametrization, it seems simpler to fold the

effects of ϕ_E and ϕ_D into the E and D values and keep the equations in their less complex form.

On the other hand, the true values of the mass entrainment and detrainment are important for comparison of LES results with field studies, or possibly for calculations of aerosol reactions whose chemical properties are dependent on the concentration of liquid water in the air (Hoppel et al. 1994). They are also vital for diagnosing mass exchanges of individual clouds in an LES ensemble, for which a simple "environment" and "cloud core" mean tracer budget may be difficult to define.

The large positive value of $w_{entrain}$ is clearly inconsistent with the often-made assumption that fluid entrained into the cloud core has negligible vertical momentum (Simpson and Wiggert 1969; Gregory 2001; Siebesma et al. 2003). This is reflected in the smaller values of the transformed E_{wT} and D_{wT} shown in Fig. 4. The negative values of w entrainment and q_t and w detrainment produced near cloud base emphasize the artificial nature of the tracer budget entrainment and detrainment. E_ϕ and D_ϕ should be interpreted simply as mathematical quantities that satisfy both the continuity equation (2) and the tracer budget of the cloud core under the assumption that the core entrains mean environment fluid and detrains mean cloud core fluid.

While the tendency for rapidly ascending shell air to be entrained more often than the slower parts of the shell was found for cloud core entrainment, we would like to emphasize that this process is not an artifact of the cloud core sampling; similar results appear when we perform entrainment calculations for simple cloudy regions (areas of condensed liquid water). In this case, vertical advection of air can drive condensation, converting environment air into cloud air, and thus driving entrainment of air into the cloud.

18

As both BOMEX and ARM model runs involved non-precipitating shallow cumulus, we have ignored the effects of precipitation. Precipitation is generally not considered part of the turbulent mixing processes associated with entrainment and detrainment in parametrization, instead being represented by a sink term in the liquid water budget (Tiedtke 1989; Kain and Fritsch 1990). Nevertheless, incorporating precipitation into the tracer budget and direct entrainment calculations would be relatively simple. The precipitation flux divergence would be a new sink/source forcing term in Siebesma's equation (3), and would be part of the forcing term $\rho \mathcal{A} S_\phi$ in Romps' equation (5), resulting in precipitation flux divergence not being counted as part of the detrainment. Specifying the advection terms would be somewhat trickier since, depending on the complexity of the microphysics scheme, moisture might be advected as a single q_t field or advected as separate hydrometeor classes. However, this would simply mean adding extra advection terms for each hydrometeor class. Once these effects were properly incorporated into the calculations, the transformations between (E_d, D_d) and (E_q, D_q) would be unchanged.

7. Conclusion

We have explained the differences between values of cloud core entrainment and detrainment of mass calculated via tracer budget and direct calculations as the result of the presence of a shell of moist air around the cloud cores and drier air at the edge of the cloud core, and the tendency for the mean tracer value of the entrained fluid to be greater than the mean tracer value of the cloud shell. Relaxing the assumption made by Siebesma and Cuijpers (1995) that entrained and detrained fluid has the properties of the environment and core,

19

respectively, allows us to transform direct entrainment/detrainment values into equivalent tracer budget values suitable for use in simple entraining plume parameterizations of cumulus convection.

The moistest, fastest-rising regions of the shell appear to be entrained more often than drier, slower-rising regions. This tendency appears to result from thermodynamic phase changes in rising air parcels. Condensation in upward moving, saturated, but negatively buoyant air parcels causes latent heating, increasing the air's buoyancy and causing it to entrain into the core. This effects suggests that the dynamics of the moist cloud shell have a role in mediating fluxes between the clouds and the environment.

Transforming directly calculated values of entrainment and detrainment into tracer budget values results in different values for total specific water q_t and liquid-water moist static energy h than for vertical velocity w. Furthermore, the tracer budget values of entrainment and detrainment compatible with q_t, h and w exhibit different patterns of variability over the course of a diurnal cycle in a GCSS ARM LES. This suggests that cumulus cloud parameterizations should use different E and D values for q_t and h than for w, and raises the possibility that different entrainment and detrainment rates apply to other cloud properties, such as aerosol concentrations.

Direct entrainment and detrainment calculations are a powerful tool that should be used to help improve our understanding of the dynamics of cloud mass exchanges, with an eye to folding these effects into the simplest parameterizations possible. Doing so has the potential to improve GCM parametrization of the magnitude and variability of mass and tracer exchanges between clouds and their environment.

APPENDIX

Table of Notation

Table 1 goes here.

REFERENCES

Bechtold, P., M. Koehler, T. Jung, F. Doblas-reyes, M. Leutbecher, M. J. Rodwell, F. Vitart, and G. Balsamo, 2008: Advances in simulating atmospheric variability with the ECMWF model: From synoptic to decadal time-scales. *Q. J. R. Meteorol. Soc.*, **134 (634, Part A)**, 1337–1351, doi:10.1002/qj.289.

Brown, A. R., et al., 2002: Large-eddy simulation of the diurnal cycle of shallow cumulus convection over land. *Q. J. R. Meteorol. Soc.*, **128**, 1075–1093.

Dawe, J. T. and P. H. Austin, 2011: Interpolation of LES cloud surfaces for use in direct calculations of entrainment and detrainment. *Mon. Wea. Rev.*, **139 (2)**, 444–456, doi: 10.1175/2010MWR3473.1.

de Rooy, W. C. and A. P. Siebesma, 2010: Analytical expressions for entrainment and detrainment in cumulus convection. *Q. J. R. Meteorol. Soc.*, **136 (650)**, 1216–1227, doi: 10.1002/qj.640.

Gregory, D., 2001: Estimation of entrainment rate in simple models of convective clouds. *Q. J. R. Meteorol. Soc.*, **127 (571, Part A)**, 53–72.

Heus, T. and H. J. J. Jonker, 2008: Subsiding shells around shallow cumulus clouds. *J. Atmos. Sci.*, **65**, 1003–1018.

Heus, T., C. F. J. Pols, H. J. J. Jonker, H. E. A. V. den Akker, and D. H. Lenschow, 2009:

23

Observational validation of the compensating mass flux through the shell around cumulus clouds. *Q. J. R. Meteorol. Soc.*, **135**, 101–112.

Hoppel, W. A., G. M. Frick, J. Fitzgerald, and R. E. Larson, 1994: Marine boundary-layer measurements of new particle formation and the effects nonprecipitating clouds have on aerosol-size distribution. *J. Geophys. Res.-Atmos.*, **99**, 14 443–14 459.

Jonas, P. R., 1990: Observations of cumulus cloud entrainment. *Atmos. Res.*, **25**, 105–127.

Jonker, H. J. J., T. Heus, and P. P. Sullivan, 2008: A refined view of vertical mass transport by cumulus convection. *Geophys. Res. Let.*, **35**, L07 810.

Kain, J. S. and J. M. Fritsch, 1990: A one-dimensional entraining/detraining plume model and its application in convective parameterization. *J. Atmos. Sci.*, **47**, 2784–2802.

Khairoutdinov, M. F. and D. A. Randall, 2003: Cloud resolving modeling of the arm summer 1997 iop: model formulation, results, uncertainties, and sensitivities. *J. Atmos. Sci.*, **60**, 607–625.

Randall, D., et al., 2003: Confronting models with data: The GEWEX cloud systems study. *Bulletin of the American Meteorological Society*, **84 (4)**, 455–469, doi:10.1175/BAMS-84-4-455, URL http://journals.ametsoc.org/doi/abs/10.1175/BAMS-84-4-455, http://journals.ametsoc.org/doi/pdf/10.1175/BAMS-84-4-455.

Rodts, S. M. A., P. G. Duynkerke, and H. J. J. Jonker, 2003: Size distributions and dynamical properties of shallow cumulus clouds from aircraft observations and satellite data. *J. Atmos. Sci.*, **60**, 1895–1912.

1 Romps, D. M., 2010: A direct measure of entrainment. *J. Atmos. Sci.*, **67 (6)**, 1908–1927.

2 Rougier, J., D. M. H. Sexton, J. M. Murphy, and D. Stainforth, 2009: Analyzing the cli-
3 mate sensitivity of the HADSM3 climate model using ensembles from different but related
4 experiments. *J. Climate*, **22 (13)**, 3540–3557, doi:10.1175/2008JCLI2533.1.

5 Siebesma, A. P., 1998: Shallow cumulus convection. *Buoyant Convection in Geophysical*
6 *Flows*, E. J. Plate, Ed., Kluwer Academic Publishers, 441–486.

7 Siebesma, A. P. and J. W. M. Cuijpers, 1995: Evaluation of parametric assumptions for
8 shallow cumulus convection. *J. Atmos. Sci.*, **52**, 650–666.

9 Siebesma, A. P., et al., 2003: A large eddy simulation intercomparison study of shallow
10 cumulus convection. *J. Atmos. Sci.*, **60 (10)**, 1201–1219.

11 Simpson, J. and V. Wiggert, 1969: Models of precipitating cumulus towers. *Mon. Wea. Rev.*,
12 **97 (7)**, 471.

13 Stainforth, D. A., et al., 2005: Uncertainty in predictions of the climate response to rising
14 levels of greenhouse gases. *Nature*, **433**, 403–406.

15 Tiedtke, M., 1989: A comprehensive mass flux scheme for cumulus parameterization in
16 large-scale models. *Mon. Wea. Rev.*, **117**, 1779–1800.

17 Wang, Y. and B. Geerts, 2010: Humidity variations across the edge of trade wind cumuli:
18 Observations and dynamical implications. *Atmos. Res.*, **97 (1-2)**, 144 – 156, doi:DOI:
19 10.1016/j.atmosres.2010.03.017.

Wu, C.-M., B. Stevens, and A. Arakawa, 2009: What controls the transition from shallow to deep convection? *J. Atmos. Sci.*, **66**, 1793–1806.

List of Tables

TABLE 1. List of Symbols

Symbol	Units	Definition	First Occurrence
$E(z)$ $D(z)$	kg m^{-3} s^{-1}	Cloud core mass entrainment/detrainment rate	(2)
$E_\phi(z)$ $D_\phi(z)$	kg m^{-3} s^{-1}	Mass entrainment/detrainment rate calculated using Siebesma tracer budget	(3a), (3b)
$e(x,y,z)$ $d(x,y,z)$	kg m^{-3} s^{-1}	Local mass entrainment/detrainment rate calculated directly from model velocity and tracer fields	(4)
$E_d(z)$ $D_d(z)$	kg m^{-3} s^{-1}	Cloud core mass entrainment/detrainment rate calculated from the horizontal sum of $e(x,y,z)$ and $d(x,y,z)$	§1
$(e\phi)(x,y,z)$ $(d\phi)(x,y,z)$	$[\phi]$ kg m^{-3} s^{-1}	Local cloud core ϕ entrainment/detrainment rate calculated directly from model velocity and tracer fields	(5)
$(E\phi)_d(z)$ $(D\phi)_d(z)$	$[\phi]$ kg m^{-3} s^{-1}	Cloud core ϕ entrainment/detrainment rate calculated from the horizontal sum of $(e\phi)(x,y,z)$ and $(d\phi)(x,y,z)$	§2
$E_{\phi,T}(z)$ $D_{\phi,T}(z)$	kg m^{-3} s^{-1}	Mass entrainment/detrainment rate calculated by transforming direct values into tracer budget values	(8a), (8a)
$E_{d,T}(z)$ $D_{d,T}(z)$	kg m^{-3} s^{-1}	Cloud core mass entrainment/detrainment rate calculated by transforming tracer budget values into direct values	§1
$\phi(x,y,z)$	$[\phi]$	Any fluid property, such as q_t (kg kg^{-1}), h (J kg^{-1}), or w (m s^{-1})	§1
$\phi_{core}(z)$	$[\phi]$	Mean cloud core ϕ	§3a
$\phi_{edge}(z)$	$[\phi]$	Mean cloud edge ϕ	§3a
$\phi_{shell}(z)$	$[\phi]$	Mean cloud shell ϕ	§3a
$\phi_{env}(z)$	$[\phi]$	Mean environment ϕ	§3a
$\phi_{entrain}(z)$	$[\phi]$	Effective value of ϕ being entrained calculated from $(E\phi)_d/E_d$	§3b
$\phi_{detrain}(z)$	$[\phi]$	Effective value of ϕ being detrained calculated from $(D\phi)_d/D_d$	§3b
$\phi_E(z)$	$[\phi]$	Placeholder for the value of ϕ assumed to be entraining	(8a)
$\phi_D(z)$	$[\phi]$	Placeholder for the value of ϕ assumed to be detraining	(8b)

List of Figures

29

4   Result of transforming direct entrainment values into equivalent w budget values. a) Mean profiles of the effective w values being entrained (black line), and detrained (dotted line), overlaid on the mean w values of the core, edge, shell and environment. The entrained and detrained w values are used to transform directly calculated values of b) entrainment and c) detrainment (grey line) into equivalent tracer budget values (black line). The entrainment and detrainment values transformed using q_t are shown for comparison (dotted lines).   33

5   Variation in a) the fraction of core air in a mixture of core and environmental air needed to produce the mean humidity entrained by the clouds, b) the fraction of environmental air in a mixture of core and environmental air needed to produce the mean humidity detrained by the clouds, c) the fraction of core air in a mixture of core and environmental air needed to produce the mean vertical velocity entrained by the clouds, and d) the fraction of environmental air in a mixture of core and environmental air needed to produce the mean vertical velocity detrained by the clouds, over the duration of the ARM model run.   34

6   Instantaneous vertical cross-section of directly calculated cloud core mass entrainment (a), humidity entrainment (b), vertical velocity entrainment (c), buoyancy (d), condensed liquid water (e), and vertical velocity (f) of a single model cloud, illustrating the tendency to entrain shell air that is rising faster than the mean shell. Black lines indicate the edge of the cloud core in each figure.   35
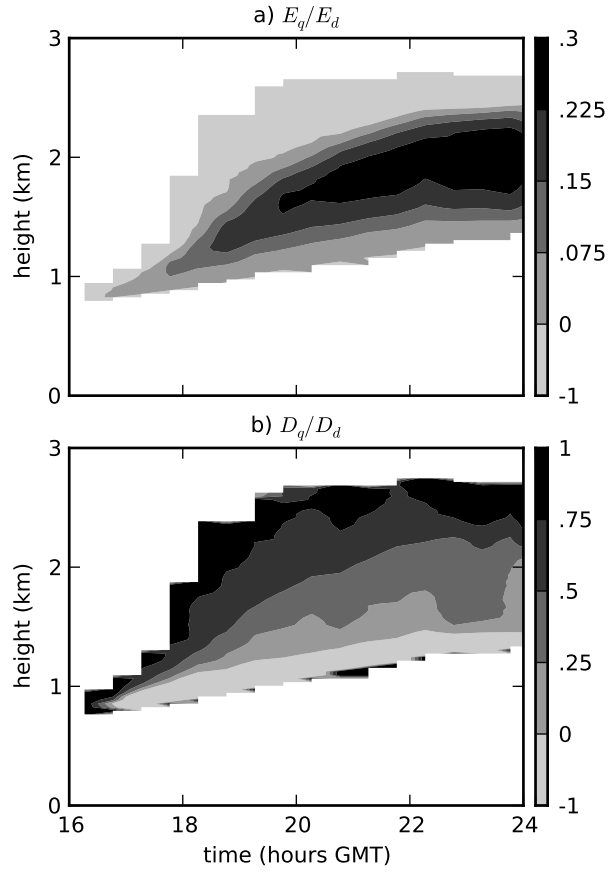
FIG. 1. Ratio of the total specific water tracer budget a) entrainment and b) detrainment values to the directly calculated values over the duration of the ARM model run.
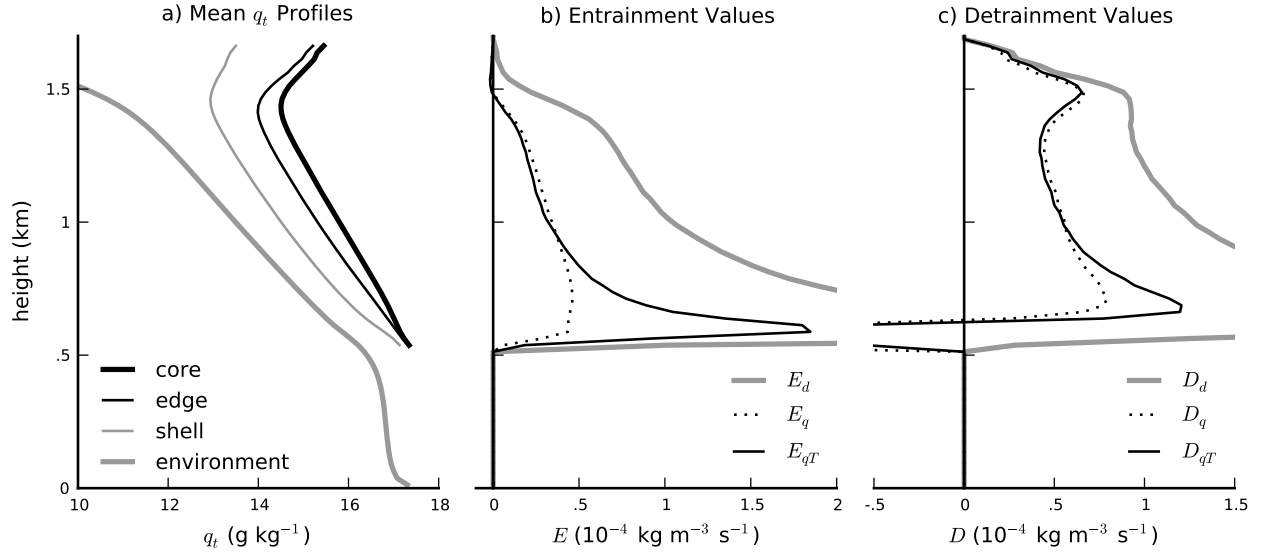
FIG. 2. Result of transforming direct entrainment values into equivalent tracer budget values using mean cloud core shell and edge properties. a) Mean profiles of the total specific humidity in the cloud core (thick black line), cloud core edge (thin black line), cloud core shell (thin grey line), and cloud core environment (thick grey line). These q_t values are used to transform directly calculated values of b) entrainment and c) detrainment (grey line) into equivalent tracer budget values (black line). The tracer budget entrainment and detrainment are shown for comparison (dotted lines).
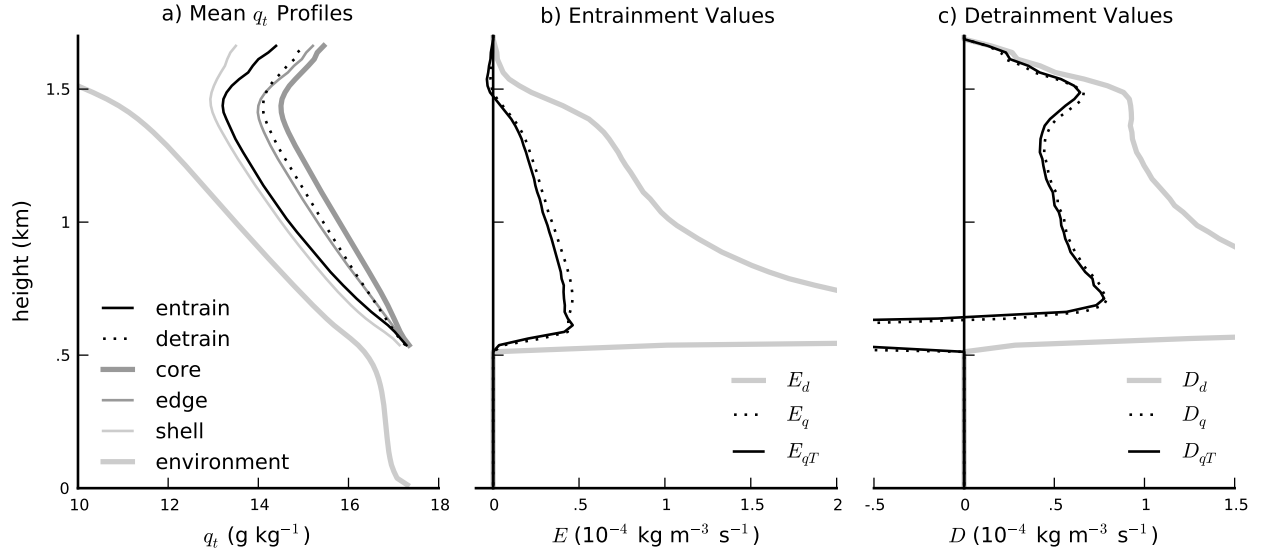
FIG. 3. Result of transforming direct entrainment values into equivalent tracer budget values using effective entrainment and detrainment properties. a) Mean profiles of the effective total specific humidity values being entrained ($q_{entrain}$, black line), and detrained ($q_{detrain}$ dotted line), overlaid on the mean total specific water values of the core, edge, shell and environment. These q_t values are used to transform directly calculated values of b) entrainment and c) detrainment (grey line) into equivalent tracer budget values (black line). The Siebesma tracer budget entrainment and detrainment are shown for comparison (dotted lines).
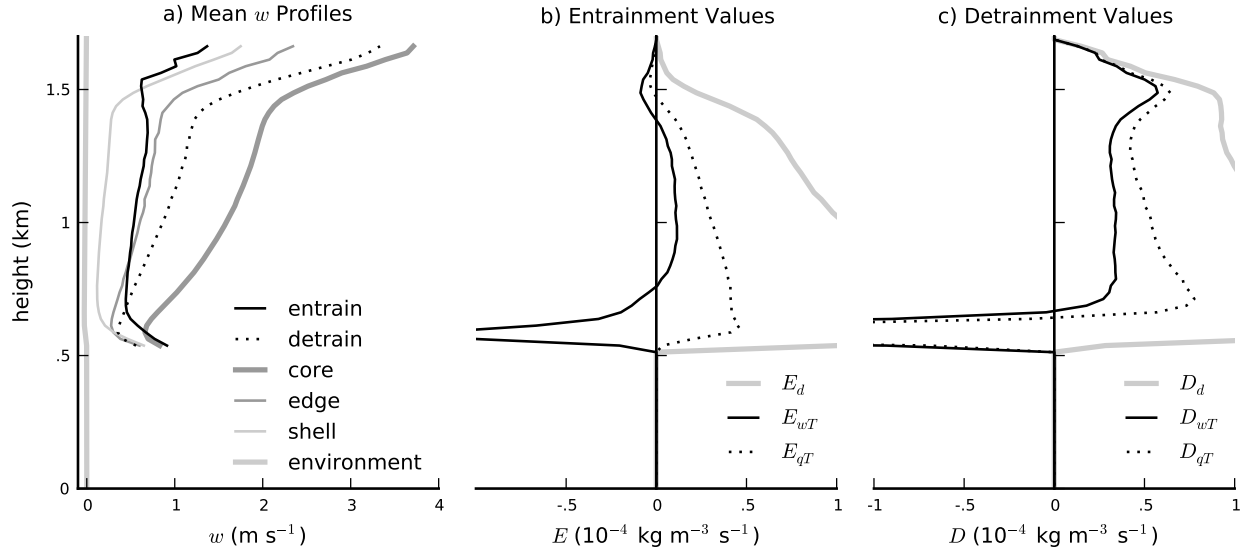
FIG. 4. Result of transforming direct entrainment values into equivalent w budget values. a) Mean profiles of the effective w values being entrained (black line), and detrained (dotted line), overlaid on the mean w values of the core, edge, shell and environment. The entrained and detrained w values are used to transform directly calculated values of b) entrainment and c) detrainment (grey line) into equivalent tracer budget values (black line). The entrainment and detrainment values transformed using q_t are shown for comparison (dotted lines).
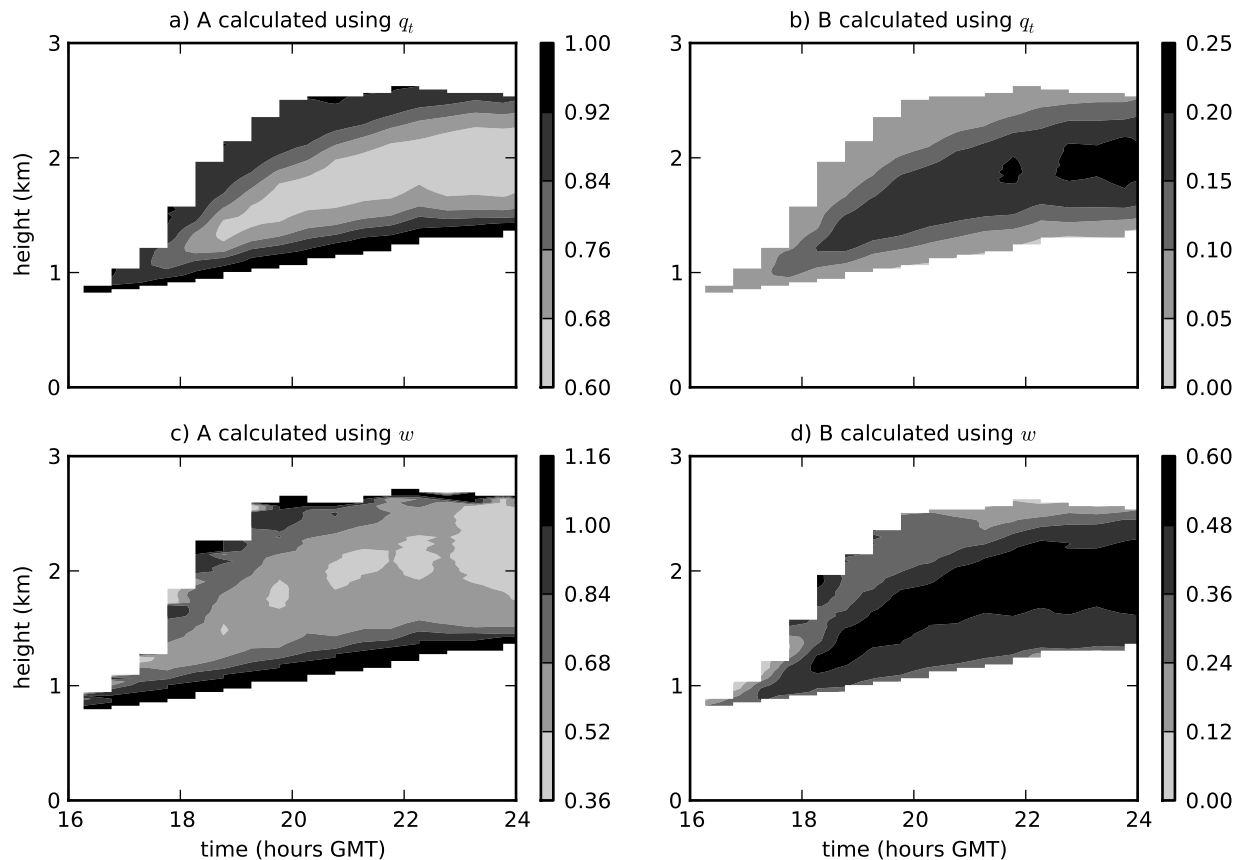
FIG. 5. Variation in a) the fraction of core air in a mixture of core and environmental air needed to produce the mean humidity entrained by the clouds, b) the fraction of environmental air in a mixture of core and environmental air needed to produce the mean humidity detrained by the clouds, c) the fraction of core air in a mixture of core and environmental air needed to produce the mean vertical velocity entrained by the clouds, and d) the fraction of environmental air in a mixture of core and environmental air needed to produce the mean vertical velocity detrained by the clouds, over the duration of the ARM model run.
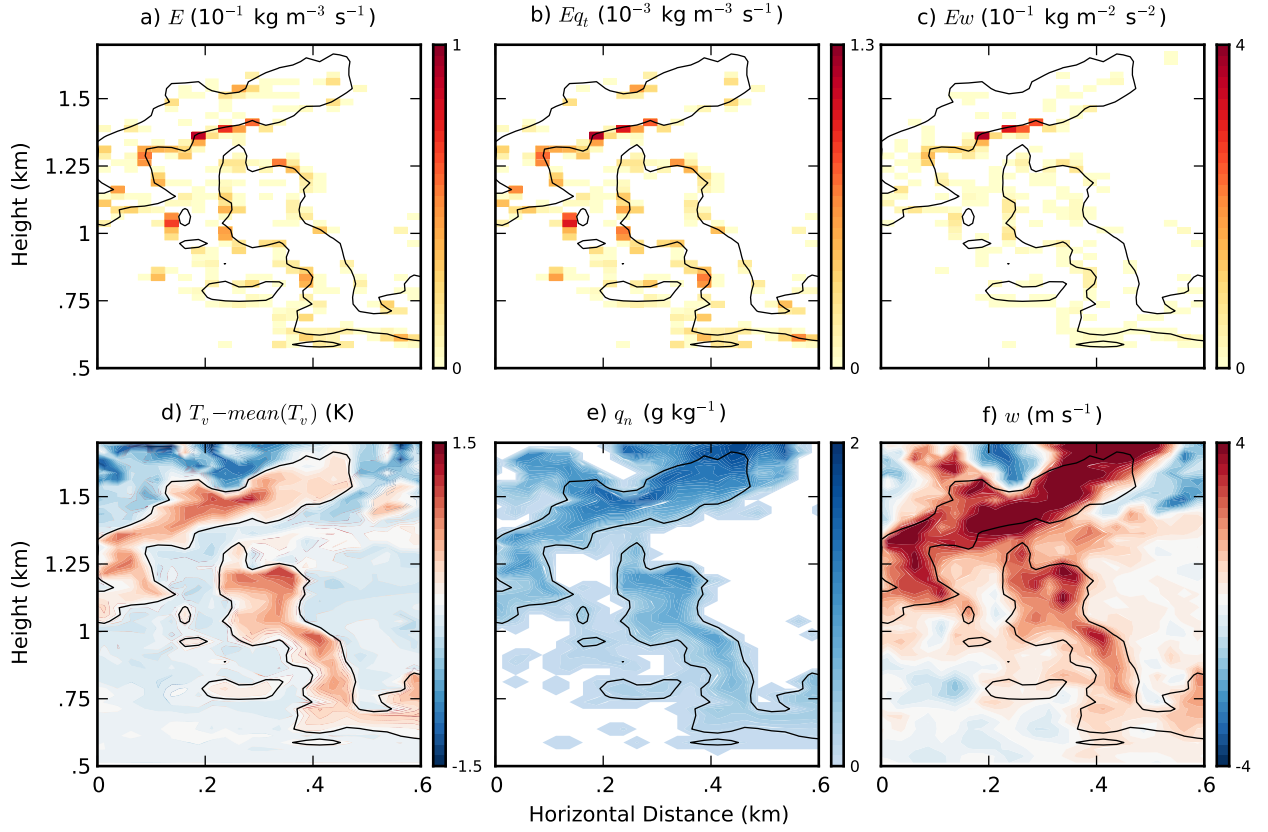
FIG. 6. Instantaneous vertical cross-section of directly calculated cloud core mass entrainment (a), humidity entrainment (b), vertical velocity entrainment (c), buoyancy (d), condensed liquid water (e), and vertical velocity (f) of a single model cloud, illustrating the tendency to entrain shell air that is rising faster than the mean shell. Black lines indicate the edge of the cloud core in each figure.